

THEORETICAL PREDICTIONS OF HYDROGEN RECOMBINATION ON ZIRCONIA

C. Bruno, F. Finamore
University of Rome “La Sapienza”, Italy

The motivation for this work was the need to estimate heat deposition due to hydrogen atoms recombination inside the nozzle for the Rubbia Fission Rocket Test Facility planned by the Italian Space Agency for the Project 242 [1]. Tungsten is assumed as the nozzle structural material because its high melting point ($T_f = 3137\text{K}$). However Tungsten must be coated because of its reactivity (hot corrosion) [2]. Among thermal barrier coatings, Zirconia has high T_f (2900 K), low reactivity, a thermal dilatation coefficient, $\alpha = 5.6 \times 10^{-6} \text{ }^{\circ}\text{C}^{-1}$, very close to that of Tungsten, ($4.98 \times 10^{-6} \text{ }^{\circ}\text{C}^{-1}$), and very low thermal conductivity, $0.77 - 1.11 \text{ W/mK}$, compared to that of Tungsten, 118 W/mK .

1-D equilibrium simulations using the NASA CEA Code 400 suggest H may recombine on the colder Zirconia walls. Since the $\text{H} + \text{H} \rightarrow \text{H}_2$ recombination is strongly exothermic ($D_{\text{eH}_2} = 436 \text{ kJ/mol}$) [3], catalysis could substantially add to the wall heat load. A model is presented here for catalytic recombination of H over ZrO_2 that follows the approach developed in [4] for O and N over sil-

ica. The recombination probability γ is defined as ratio between flux of atoms recombining at surface and flux of atoms impinging at surface. The flux of impinging particles (atoms/molecules) is determined in these models from the kinetic theory of gases:

$$Z_p = \frac{p_p}{\sqrt{2\pi m_p k T}} \quad (1)$$

The fraction of impinging particles adsorbed is proportional to the sticking coefficient, s : $Z_{\text{adsorbed particles}} = s Z_{\text{impinging particles}}$; s depends on the probability to strike a free site. The coverage coefficient θ (ratio between number of filled sites and number of sites) is a measure of the probability that a site is occupied by an atom.

The gas atoms adsorption probability depends on the sticking coefficient s_a .

In the case of molecules, adsorption is modeled as to depend on an activation energy E_a , and a steric factor P_m accounting for the trajectory of the molecule impacting the surface.

The flux of adsorbed atoms is

$$Z_{A,aA} = s_a (1 - \theta) Z_A \quad (2)$$

and that of adsorbed molecules

$$Z_{A,aM} = 2 \left(1 - \theta\right)^2 \underbrace{P_m e^{-E_a/RT}}_{s_m} Z_M \quad (3)$$

Following adsorption, atoms recombine to molecules through an Eley-Rideal reaction, E-R, and their recombination flux is

$$Z_{A,dER} = \theta Z_A P_{ER} e^{-Q_{ER}/RT} \quad (4)$$

with P_{ER} accounting for impact orientation and other unknowns, and through a Langmuir-Hinshelwood reaction, L-H, when two ad-atoms have sufficient energy to move on the surface and collide forming diatoms. Its flux of recombined atoms is:

$$Z_{A,dLH} = 2 N_m = v N \theta^2 e^{-Q_{LH}/RT} \quad (5)$$

The flux of molecules desorbing, N_m , depends on the number of collisions N_{coll} (per unit time and area)

$$N_{coll} = \frac{1}{2} \underbrace{\frac{v}{D}}_{v} \underbrace{N \theta^2 e^{-E_m/RT}}_{\text{Number of Mobile Adatoms}} \quad (6)$$

$$N_m = N_{coll} e^{-Q_{LH}/RT} \quad (7)$$

Because ad-atoms must have energy greater than E_m to move on the surface, the frequency of collisions in (6) is assumed as the ratio between the mean velocity of mobile ad-atoms, v_{A^*} , and the distance between two adjacent sites, Δ . For a two-dimensional gas the velocity v_{A^*} is:

$$v_{A^*} = \sqrt{\frac{\pi k T}{2 m_A}} \quad (8)$$

In (7), the activation energy Q_{LH} is the larger between E_m and Q_{lh} .

Following E-R or L-H recombination, the molecule can desorb. Ad-atoms with sufficient energy can leave the surface without recombining (thermal desorption). Its flux is:

$$Z_{A,dTH} = N \theta \frac{kT}{h} e^{-Q_a/RT} \quad (9)$$

The total flux of ad-atoms desorbing as recombined molecules is therefore

$$Z_{A,REC} = Z_{A,Aa} - Z_{A,dTH} + Z_{A,dER} \quad (10)$$

and since

$$Z_{A,REC} = \gamma (Z_A + 2 Z_M) \quad (11)$$

equating (10) and (11), together with the flux expressions (2), (4), (9), yields the γ sought

$$\gamma = s_a (1 - \theta) - \frac{NkT}{Z_A h} e^{-Q_a/RT} \theta + \gamma^* \theta \quad (12)$$

In Eq.(14), the factor γ^* represents the micro probability of a successful formation of the molecule when an atom from the gas strikes an ad-atom, expressed as:

$$\gamma^* = P_{ER} e^{-Q_{ER}/RT} \quad (13)$$

The coverage coefficient θ in (12) is calculated assuming a steady-state dynamical equilibrium, between adsorption and desorption:

$$\begin{aligned} Z_{A,ads} &= Z_{A,des} \Rightarrow \\ \Rightarrow Z_{A,aA} + Z_{A,aM} &= Z_{A,dLH} + Z_{A,dER} + Z_{A,dTH} \end{aligned} \quad (14)$$

Substituting the expression of the fluxes (2), (3), (4), (5), (9) on the right and left term of (14), the equation for θ to solve together with (12) for γ is

$$\begin{aligned} s_a (1 - \theta) + 2 \frac{Z_M}{Z_A} s_m (1 - \theta)^2 &= \gamma^* \theta + \\ + \frac{vN}{Z_A} e^{-Q_{LH}/RT} \theta^2 + \frac{N}{Z_A} \frac{kT}{h} e^{-Q_a/RT} \theta & \end{aligned} \quad (15)$$

Estimating Catalytic Model Parameters

Predictions using (12) and (15) require knowledge of several energy parameters.

The interaction forces between Zirconia and Hydrogen depend on the crystal structure of Zirconia. The layers of crystal atoms most influential on an ad-atom are assumed as “the surface”. The crystal structure of Zirconia is a face-centered cube of Zirconium atoms, enclosing a cube of Oxygen atoms. The crystal plane <111> is assumed as the exposed face that interacts with the gas. The Zirconia surface can be visualized as a layer of Zirconium coated by an Oxygen cloud both interacting with impinging Hydrogen atoms: H tends to bind with O rather than with Zr [5, 6].

Catalytic “sites” are defined as locations where H atoms are fully chemisorbed (i.e., where the H interaction potential with the surface is lowest).

The parameters (Q_{LH} , Q_{ER} , E_m , Q_a , v) in Eqs. (12) and (15) depend on site locations and on the minimum interaction potential among ad-atom and crystal; both are calculated by carefully defining the crystal structure and first crystal layer impacted by the gas particles. The total Hydrogen-surface potential must be calculated by adding the contributions of the most influential crystal atoms along the surface and in the sublayers.

The potential assumed here is the Morse potential [7]. Taking advantage of its additive property, the Hydrogen Morse potential due to the surface, first layer and more influent sublayers is assumed as the sum of single H(gas) – O (crystal) pairs.

The Morse potential can be calculated knowing the three parameters B_e , D_e , ω_e that can be found for instance from spectral analysis [8]. The Morse potential for a single pair of atoms is:

$$V(x) = D_e \left[\left(1 - e^{-bx} \right)^2 - 1 \right] \quad (16)$$

So, the potential of a Hydrogen ad-atom due to its surface interaction is:

$$V_H(x) = \sum V_{OH} + \sum V_{ZrH} \quad (17)$$

The sums should include all lattice atoms, however, generally, the first three layers of the surface are found the most influential.

The potential of O-H pairs is also affected by Zirconium atoms. A review of spectra literature did not find information on the bond energy of ZrO-H; consequently, this parameter is calculated by applying the Hess law.

The D_e of ZrO-H is equal to the enthalpy of the reaction $ZrOH(g) = ZrO(g) + H(g)$.

The D_e of ZrO-H so calculated as $D_{e(O-H)} = 190.2$ kJ/mol implies the Zirconium atom weakens the O-H bond that, without Zr, would be 427.8 kJ/mol [9]. The other parameters sought are: $r_{e(O-H)} = 0.96 \text{ \AA}$ [3], B_e , and $\omega_{e(O-H)} = 3660 \text{ cm}^{-1}$ [10]. The Morse parameter for ZrH are $r_{e(Zr-H)} = 1.77 \text{ \AA}$ and $\omega_{e(Zr-H)} = 1777 \text{ cm}^{-1}$ [11].

Applying again the Hess law, the enthalpy of reaction $ZrH(g) = Zr(g) + H(g)$ is assumed equal to Zr-H bond energy, and therefore $D_{e(Zr-H)} = 300.8$ kJ/mol.

The potentials V_{ZrH} and V_{OH} in Eq.(17) are then written by substituting the two sets of parameters (r_e , D_e , ω_e) just found inside Eqs. (16). Which surface atoms affect V_H is estimated by comparing the V_{ZrH} and V_{OH} calculated for several O-H and Zr-H pairs along the same layer and varying the layer. In summary, the

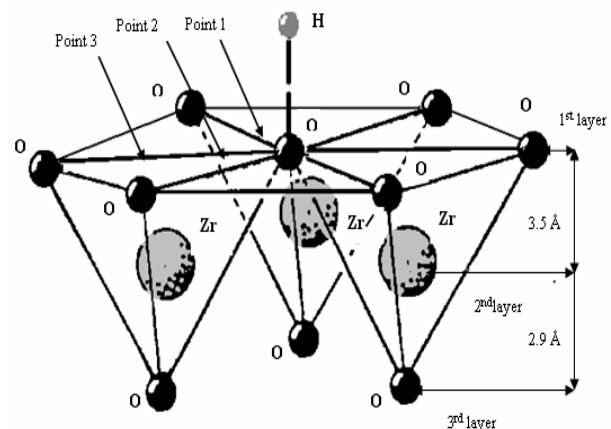


Fig.1 Configuration of the most influential atoms shaping V_H (elementary cell)

configuration of the most influential atoms is found to depend on three surface layers, as sketched in Fig.1:

This configuration is assumed as the elementary cell to calculate V_H , adding the contribution of all three layers. The minimum of $V_H(x)$ (- 391.424 kJ/mol, at $r_e = 0.93 \text{ \AA}$) corresponds to a likely adsorption site. Local minima $V_{H\min}$ must be calculated at every surface location of H, the lowest corresponding to the H adsorption state.

We assume that the lowest $V_{H\min}$ lies on line between two adjacent O atoms on the first layer (they are the closest to H).

Looking at Fig.1, successive $V_{H\min}$ were calculated by moving H along the shortest path between two O atoms on the first layer.

Besides the point 1 just evaluated other significant locations are point 2, at $r_e = 0.93 \text{ \AA}$ from the nearest O, and point 3, in the middle of the O-O path, at the distance 1.75 \AA from both nearest O atoms. At both these points the most influential crystal atoms are found by adding other elementary cells to that shown in Fig. 3; which Zr and O of the cluster influence more V_H is determined by comparing V_{OH} and V_{ZrH} . The $V_{H\min}$ turn out to be -259.865 kJ/mol at point 2, and -483.209 kJ/mol at point 3. The conclusion is that this last is the deepest potential well and that the sites are located in the middle of the line joining two adjacent O atoms located on the first layer, with adsorption energy $Q_a = -V_{H\min 3} = 483.209 \text{ kJ/mol}$. Therefore the minimum distance between two sites is $\Delta = 1.75 \text{ \AA}$, hence their density $N = 6.28 \times 10^{18} \text{ m}^{-2}$. Furthermore, the migration energy, E_m , equal to the difference between the adsorption energy and the maximum $V_{H\min}$, is found to be $E_m = 223.344 \text{ kJ/mol}$.

Application of the Model to the Hydrogen/Zirconia case

Some of the assumptions in [12] are kept and other will be relaxed in applying

the model just presented to H/ZrO₂ recombination.

Assume, for the time being only, that there is complete chemical energy accommodation (CEA), $\beta=1$ and that the nozzle cooling system maintains its surface temperature uniform, $T_{\text{wall}} = 1000 \text{ K}$. The flux in the nozzle is assumed isentropic, in thermochemical equilibrium and chocked at the throat.

To determine γ the Q_{ER} and Q_{LH} in the adsorption and desorption fluxes must be calculated using the result just found.

The flux of adsorbed H modeled by Eqs. (1) and (2) depends on s_a , a parameter not found in the literature. The flux of adsorbed H₂ is from Eq. (3). Dissociative adsorption of H₂ may occur, because the minimum distance between two Zirconia sites ($\Delta=1.75 \text{ \AA}$) is close to the diameter of H₂ (1.48 \AA , in the ground state) [3].

Assuming $E_a = 0$ in Eq. (3), P_m is equal to s_m ; again, there are no literature data on s_m and P_m for H₂ adsorption on ZrO₂. So, P_m (or s_m) and s_a are missing parameters in modelling adsorption fluxes. These fluxes depend also on the p_H and p_{H_2} pressures at the wall requiring complete knowledge of the nozzle gas dynamic field. If it is reasonable to assume the pressure roughly uniform on the nozzle cross section, then $p(x)_{\text{wall}} = p(x)_{\text{axis}}$.

The quantities $p(x)_{\text{axis}}$, $n_i(x)_{\text{axis}}$, $T(x)_{\text{axis}}$ are calculated using the 1-D NASA CEA400 code, from the nozzle geometry (entrance diameter = 40 cm, throat diameter = 0.977 cm, $A_e/A_t = 476$) and from the nozzle stagnation conditions ($p_i=6 \text{ atm}$, $T_i = 9500 \text{ K}$)[13].

The solution shows that molar fraction n_H decreases along x while n_{H_2} increases, with n_H always $\gg n_{H_2}$. On the wall molar fractions depend on the ratio between diffusion time to the wall and recombination time of $H + H + M \rightarrow H_2 + M$.

Short of solving for the complete 3-D Navier Stokes equations describing this nozzle flow, two extreme cases are chosen to bracket the solution: equilibrium, and frozen flow.

Wall and axis molar fractions are equal in the frozen case, while for equilibrium the NASA CEA400 code predictions show that the wall molar fraction of H₂ is almost one. The partial pressures at the wall are calculated for these two extreme cases and so is adsorption.

To calculate the flux of particles released by recombination (E-R and L-H) and by thermal desorption, the unknown parameters are: Q_{ER}, Q_{LH}, thermal desorption energy, P_{ER} and s_a.

The E-R mechanism is frequently a non-activated process: in many cases the bond energy of the recombined molecule is greater than that of the ad-atom. However in the case of H on Zirconia the bond energies are D_{eH2(gas)} = 436 kJ/mol < D_{eH(ad-atom)} = 483.209 kJ/mol. So

$$Q_{ER} = \nabla E = V[H_2(gas)] - V[H(ad-atom)] = -436 - (-483.209) = 47.209 \text{ kJ/mol} \quad (18)$$

must be surmounted to activate E-R recombination. In fact, 47.209 kJ/mol is the highest possible value of Q_{ER}: the real E-R recombination barrier could be lower, as E-R recombination may occur even though the ad-atom is not yet at the bottom of the potential well [14], or when a fraction of the energy barrier is supplied by wall phonons excited by a previous recombination at the same site.

L-H recombination is instead an activated process; in fact, it occurs only at temperatures higher or much higher than those typical of E-R. The energy barrier Q_{LH} is the larger between E_m and Q_{lb}: Q_{LH} = 2Q_H - D_{eH2} = 530.418 kJ/mol. Eq. (5) for the flux Z_{A,dLH} assumes collisions between two mobile ad-atoms: whether this may occur for H(ad-atom) on Zirconia needs verification. At T_w = 1000 K the fraction N_{ads-free} of mobile ad-atoms, assuming θ = 1, is equal to:

$$\frac{N_{H\,ads-free}}{N_{H\,ads}} = e^{-E_m/RT} = 2 \times 10^{-12} \quad (19)$$

Thus the fraction of mobile ad-atoms is so low that the most probable scenario for L-H recombination is a collision between a mobile

and a trapped ad-atom. Consequently in Eq. (6) the right term must be multiplied by two (two mobile H ad-atoms to cause two collisions); this changes also the right hand side of Eq.(5).

Lastly, Q_a and N, the parameters to calculate the flux Z_{H,dTH} of atoms due to thermal desorption (9), are known.

All fluxes modeled must be substituted in Eq.(12) and (15) to calculate θ and the probability of recombination γ.

Because Q_{ER}, P_m, P_{ER}, s_a are unknown, it is not possible to calculate immediately θ and γ. This lack information can be partly compensated by exploring a suitable range of variation of these parameters, to obtain engineering “margins”.

Furthermore, as noted, adsorption fluxes are calculated in two extreme cases (frozen flow, equilibrium flow). In conclusion, an “exact” solution of the problem cannot be determined at this time, but the range of γ can.

Analysis of the Dependence of γ on Parameters

The dependence of γ on one of the unknown parameters is investigated by fixing the remaining three; the throat flow is still assumed frozen. Figs. 2, 3, 4 show the dependence of γ_H on s_a, P_m and P_{ER} respectively, assuming Q_{ER} = 47.209 kJ/mol. Fig. 5 shows the dependence of γ_H on Q_{ER}.

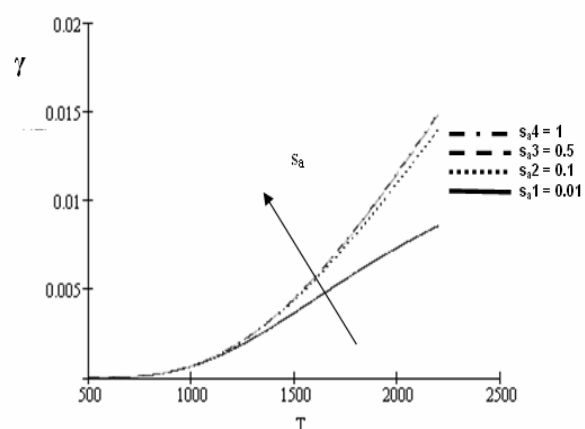


Fig.2 Dependence of γ_H on the sticking coefficient (Q_{ER} = 47.209 kJ/mol, P_m=1, P_{ER}=1)

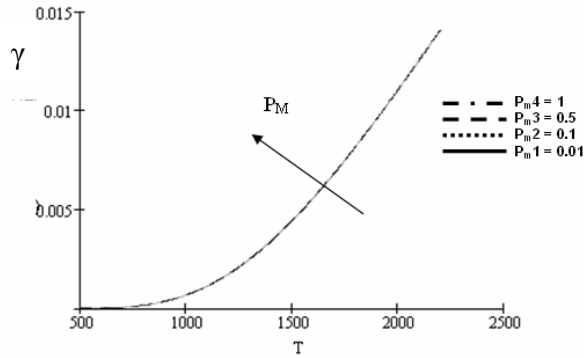


Fig.3 Dependence of γ_H on the molecular steric factor P_m ($Q_{ER} = 47.209 \text{ kJ/mol}$, $P_{ER}=1$, $s_a=1$)

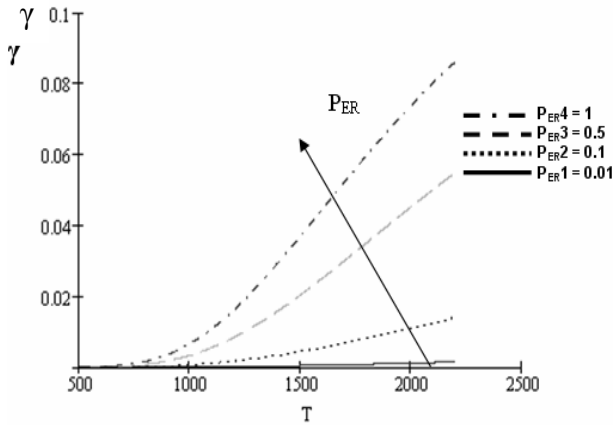


Fig.4 Dependence of γ_H on the Eley-Rideal steric factor P_{ER} ($Q_{ER} = 47.209 \text{ kJ/mol}$, $P_m=1$, $s_a=1$)

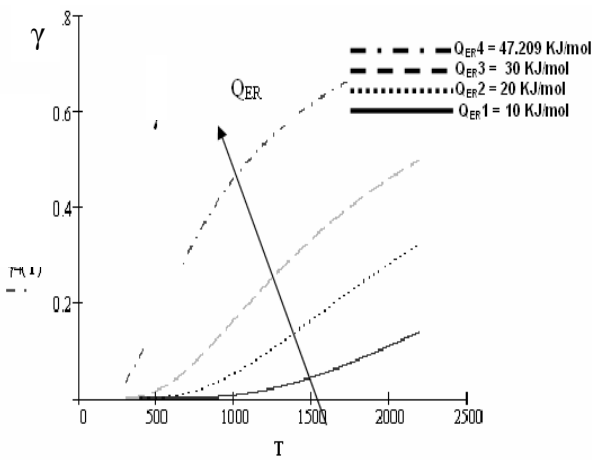


Fig.5 Dependence of γ_H on the Eley-Rideal activation energy Q_{ER} ($P_m=1$, $P_{ER}=1$, $s_a=1$)

Figs. 2 and 3 show that at wall temperature $T = 1000\text{K}$ γ_H is only weakly affected by s_a and P_m , suggesting these two parameters are less significant in influencing γ_H , and could be assumed, for instance, unity without prejudicing main results and conclusions. Also such assumption is conservative in designing a nozzle that must withstand heat loads of order up to $O(10^8) \text{ MW/m}^2$.

Results and Discussion

The recombination probability γ_H along nozzle axis x is calculated assuming s_a and P_m equal to 1, and two extreme gas flow cases (frozen or equilibrium).

In both γ_H is calculated by varying Q_{ER} (from 10 kJ/mol to 47.209 kJ/mol) and P_{ER} (from 0.01 to 1). Overall, calculations show that γ_H does not change significantly from the throat to the nozzle exit, see Table 1 (equilibrium case).

Table 1 γ_H at nozzle throat and at nozzle exit (as a function of P_{ER} and Q_{ER}). Equilibrium case. $T_W=1000\text{K}$.

Q_{ER} [kJ/mol]	$P_{ER}=0.01$		$P_{ER}=0.5$		$P_{ER}=1$	
	$Ax/At=1$	$Ax/At=476$	$Ax/At=1$	$Ax/At=476$	$Ax/At=1$	$Ax/At=476$
47.209	3.438×10^{-5}	3.566×10^{-5}	1.712×10^{-3}	1.721×10^{-3}	3.422×10^{-3}	3.422×10^{-3}
30	2.715×10^{-4}	2.752×10^{-4}	0.014	0.014	0.027	0.027
20	9.032×10^{-4}	9.098×10^{-4}	0.045	0.045	0.09	0.09
10	3.005×10^{-3}	3.018×10^{-3}	0.15	0.15	0.3	0.3

γ_H behaves similarly for the frozen case.

Table 2 γ_H at nozzle throat and at nozzle exit (as a function of P_{ER} and Q_{ER}). Frozen case. $T_W=1000\text{K}$.

Q_{ER} [kJ/mol]	$P_{ER}=0.01$		$P_{ER}=0.5$		$P_{ER}=1$	
	$Ax/At=1$	$Ax/At=476$	$Ax/At=1$	$Ax/At=476$	$Ax/At=1$	$Ax/At=476$
47.209	6.841×10^{-5}	6.841×10^{-5}	3.415×10^{-3}	3.412×10^{-3}	6.818×10^{-3}	6.809×10^{-3}
30	5.419×10^{-4}	5.418×10^{-4}	0.027	0.027	0.053	0.052
20	1.803×10^{-3}	1.802×10^{-3}	0.086	0.085	0.166	0.161
10	5.99×10^{-3}	5.982×10^{-3}	0.261	0.252	0.462	0.443

Before commenting the γ results, it is necessary to compare the gas diffusion and heterogeneous catalysis times, to find when the heat flux due to heterogeneous catalysis is dominant.

The Damköhler number for catalysis, $Da_W = \tau_{dif}/\tau_{hc}$ [15], becomes for the chemical species i :

$$Da_{Wi} = \frac{K_{Wi} Y_i}{D_{mi} (\nabla Y_i)_W} \quad (20)$$

K_{Wi} is the catalyticity that can be written, from the Hertz-Knudsen relation [16]

$$K_{Wi} = \gamma \sqrt{\frac{k T_w}{2 \pi m_i}} \quad (21)$$

When $Da_{Wi} \gg 1$, the contribute of heterogeneous catalysis to surface heat flux must be accounted for; when $Da_{Wi} \ll 1$ this contribute is negligible with respect to that of diffusion.

In the equilibrium case, Hydrogen close to the wall is mostly molecular, therefore $D_{WH} \ll 1$ is to be expected for the whole range of Q_{ER} and P_{ER} .

As Q_{ER} decreases and P_{ER} increases, Da_{H2} increases, because the larger γ_H (shown in Table 1) means τ_{hc} is shorter.

Catalyticity is substantial ($Da_{WH2} \gg 1$) when the activation energy Q_{ER} is low (10 kJ/mol) and $P_{ER} \geq 0.01$; quantitatively, the contribute of catalysis to surface heat flux must be included when $\gamma \approx O(10^{-1})$.

Table 1 shows γ may be assumed constant along the wall (once Q_{ER} and P_{ER} have been assumed); and any location on the nozzle wall could be used to calculate γ .

However D_{WH2} decreases moving from the throat to the nozzle exit, therefore γ at the throat is the parameter of choice to predict the magnitude of catalytic heating.

Figs. 6 and 7 show γ_H at the throat, for $T_w = 1000K$, $s_a = P_m = 1$, equilibrium or frozen

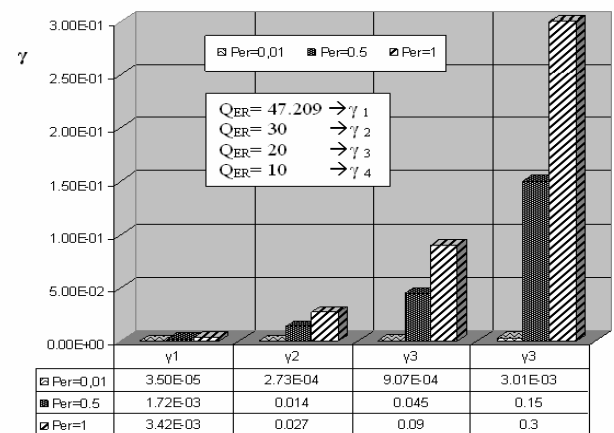


Fig.6 Dependence of γ on P_{ER} and Q_{ER} (thermochemical equilibrium assumed)

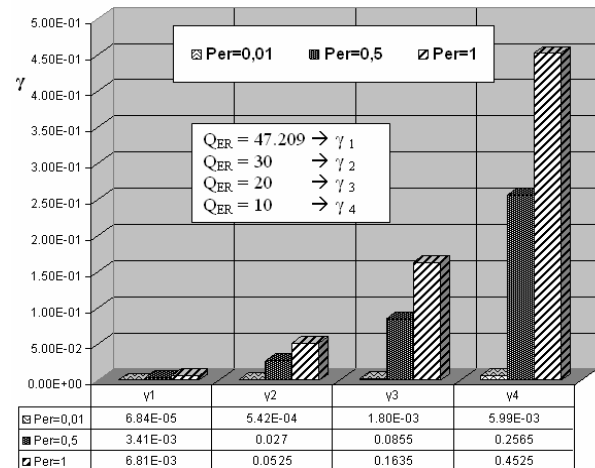


Fig.7 Dependence of γ on P_{ER} and Q_{ER} (frozen flow)

conditions, and for different values of the parameters Q_{ER} (47.209, 30, 20, 10 kJ/mol) and P_{ER} (1, 0.5, 0.01). These plots show that γ_H covers a wide range.

Therefore the spread (or rather uncertainty) on γ_H predicted suggests Zirconia might be questionable as Tungsten coating.

Chemical Energy Accommodation

This said, the fraction of the heat load due to surface recombination does not depend only on γ , but also on the CEA coefficient β , so far assumed unity. The fraction β of recombination does not depend only on γ , but also on

the CEA coefficient β , so far assumed unity. The fraction β of recombination energy released to surface is [17]:

$$\beta = \frac{2 \dot{q}}{D_e Z_{A,REC}} \quad (22)$$

Exact β predictions require predicting the energy states of the molecule recombined. Estimating β is easier if which recombination mechanism dominate is known. β depends on the residence time of recombined molecule on the surface. For L-H recombination this residence time is longer than in the case of E-R recombination [14, 17-19], consequently it seems plausible to assume $\beta_{LH} \approx 1$ and $\beta_{ER} < 1$.

θ depends likewise on the recombination mechanism: $\theta \sim 1$ or $\theta < 1$ depending on when most efficient whether E-R or L-H is the domi-

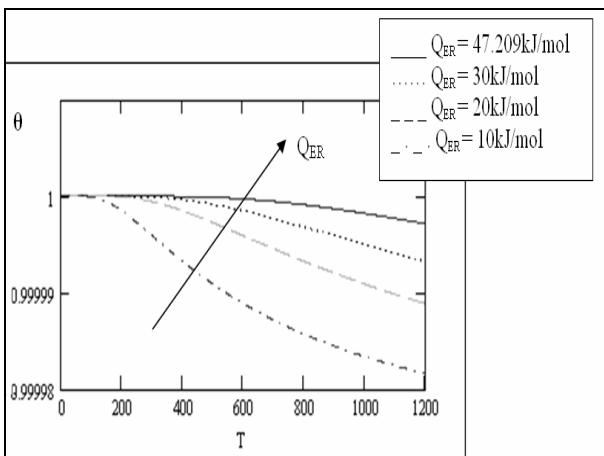


Fig.8 θ vs. temperature (equilibrium case)

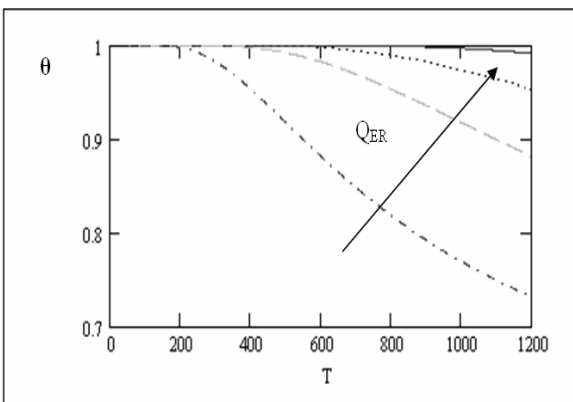


Fig.9 θ vs. temperature (frozen case)

nant mechanism. The trend of θ is calculated in the present nozzle case assuming $P_m = s_a = P_{ER} = 1$. The results are shown in Figs.8 and 9:

Whether equilibrium or frozen, at $T = 1000\text{K}$, θ is almost equal to 1, implying E-R is the main recombination mechanism and consequently $\beta < 1$. The low β means that also in the worst case ($\gamma = 0.45$) a significant fraction of recombination heat is trapped in the desorbing molecule and not deposited on the surface. Since at $T_w = 1000\text{ K}$ the main mechanism is E-R, approximating β with β_{min}

$$\beta_{min} = \frac{Q_a (1 - \theta)}{\gamma D_e / 2} \quad (23)$$

is reasonable[17]. So, at $T = 1000\text{ K}$, and $\gamma = 0.45$ (and for thermochemical equilibrium flow, $Q_{ER} = 10\text{kJ/mol}$ and $P_{ER}=1$), the coverage θ is ≈ 0.999 ; applying Eq.(23) the β predicted, $\beta \sim 8 \times 10^{-5}$, is very low. So, although the maximum γ is high (almost half of the impinging particles recombine), the actual fraction of energy deposited on the surface is negligible. The throat heat flux due to catalysis is then calculated (applying the Eq. (22)) as

$$\dot{q} = \beta_{min} \left(\frac{Z_{A,REC} D_{eH2}}{2} \right) \quad (24)$$

and is $\sim 0.42\text{ MW/m}^2$. In [2], the throat wall thermal load due to diffusion and conduction was calculated $\sim 50\text{MW/m}^2$: so, surface catalysis contributes only to $\sim 1\%$ of diffusion and conduction.

Conclusions

The total surface heat load has been estimated by developing a heterogeneous catalysis model based on [4].

The Zirconia structure has been characterized in a simple way and the interactions between H and surface atoms have been studied and modeled by calculating the appropriate energy barriers.

The influence of missing parameters (Q_{ER} , P_m , P_{ER} , s_a) on γ has been studied, showing that,

at wall $T = 1000K$, γ_H is weakly affected by s_a and P_m . The recombination probability has been calculated by varying Q_{ER} and P_{ER} and for two extreme kinetics cases (frozen or equilibrium).

Diffusion and heterogeneous chemistry characteristic times have been compared to find when the heat flux due to heterogeneous catalysis is dominant: results indicate catalysis contributes significantly only when $\gamma \sim O(10^{-1})$.

At the critical nozzle throat location, catalytic recombination is found high (~50%) and due mainly to the E-R mechanism. However, most of the catalytic recombination heat is trapped in desorbing molecule since $\beta << 1$. Thus, for the conditions examined, the contributions of heterogeneous catalysis to the wall heat flux are predicted very low compared to those due to diffusion and conduction.

At the current state of the art, experimental data on TPS catalytic behavior cannot yet be replaced with data calculated using models; however, the high cost of testing requires a careful preliminary screening of materials to test. This screening may be made easier models such as that used in this work.

References

- [1] Augelli M. et al. *Report of the Working Group on a Preliminary Assessment of a New Fission Fragment Heated Propulsion Concept and its Applicability to Manned Missions to the Planet Mars (Project 242)*. Agenzia Spaziale Italiana, Roma, 15 March 1999.
- [2] Buffone C., Bruno C. Nozzle cooling in the future Rubbia's engine Test Facility. *23rd International Symposium on Space Technology and Science*, Tokyo, ISTS Paper 2002-c-1, May 26 - June 2, 2002.
- [3] Atkins P.W., Beran J.A. *General Chemistry, Second Edition*. Scientific American Library, New York, U.S.A., 1992. p.320-325.
- [4] Barbato M., Bruno C., Nasuti F. Material-dependent catalytic recombination modeling for hypersonic flows. *Journal of thermophysics and heat transfer*, Vol.10, No. 1, pp. 131-136, Jan-Mar. 1996.
- [5] Merle-Méjean T., Barberis P., Ben Othmane S., Nardou F., Quintard P.E. Chemical Forms of Hydroxyls on/in Zirconia: An FT-IR Study. *Journal eur. ceram. soc.*, Vol.18, No.11, pp 1579-1586, 1998.
- [6] Trunschke A., Hoang D.L., Lieske H. In situ FTIR Studies of High-temperature Adsorption of Hydrogen on Zirconia. *J. chem. soc. faraday Trans.*, Vol. 91, No. 24, pp. 4441-4444, 1995.
- [7] Morse P. M. Diatomic molecules according to the wave mechanics. ii. Vibrational levels. *Phys. rev.*, Vol. 34, pp. 57-64, 1929.
- [8] Gaydon A.G. *Dissociation Energies*. Chapman and Hall, London, 1953, p.30.
- [9] Chase M.W. Jr. et al. *JANAF Thermochemical Tables*. 3rd. edn., *J. phys. chem. Ref. Data*, 14, supplement no. 1, 1985.
- [10] Morterra C., Cerrato G., Ferroni L. Surface Characterization of Yttria-stabilized Tetragonal ZrO_2 Part 1. Structural, Morphological, and Surface Hydratation Features. *Mat. chem. phys.* Vol. 37, pp. 243-257, 1994.
- [11] Balasubramanian K., Wang J.Z. Spectroscopic Properties and Potential Energy Curves of Thirty-Six Electronic States of ZrH . *Chem. phys lett.*, Vol. 154, pp. 525-530, 1989.
- [12] Buffone C., Bruno C., Sefiane K. Liquid Metal Heat Pipes for Cooling Rocket Nozzle Walls. *39th AIAA/ASME/SAE/ASEE Joint Propulsion Conference and Exhibit*, Huntsville, Alabama, AIAA-2003-4452, July 20-23, 2003.
- [13] Buffone C., *Scambio di calore in ugelli supersonici ad alte temperature*, Master Thesis, DMA, University of Rome "La Sapienza", 2000.
- [14] Kratzer P., Breing W. Highly Excited Molecules from Eley-Rideal Reactions. *Surface science*, Vol. 254, pp. 275-280, 1991.
- [15] Barbato M., Reggiani S., Bruno C. and Muylaert J. Model for Heterogeneous Catalysis on Metal Surfaces with Application to Hypersonic Flows. *Journal of thermophysics and heat transfer*, Vol. 14, No. 3, pp. 412-420, July-September 2000.
- [16] Bruno C. *Real Gas Effects*. In: Periaux J., Bertin J.J., Glowinski R., editors, "Hypersonics", Birkhäuser Boston, pp. 303-354, 1989.
- [17] Halpern B., Rosner D.E. Chemical Energy Accommodation at Catalyst Surface. *Chem. soc. faraday trans. I*, Vol. 74, pp. 1883-1912, 1978.
- [18] Masel R.I. *Principles of Adsorption and Reaction on Solid Surfaces*. John Wiley and Sons, Inc. New York, 1996.
- [19] Tully J. Dynamics of Gas-Surface Interactions: Reaction of Atomic Oxygen with Adsorbed Carbon on Platinum. *J. chem. phys.*, Vol. 73, pp. 6333-3642, 1980.